Available online at www.sciencedirect.com
SCIENCE DIRECT
Journal of Volcanology and Geothermal Research 149 (2006) 312–328
Journal of volcanology and geothermal research
www.elsevier.com/locate/jvolgeores

The role of regional-scale faults in controlling a trapdoor caldera, Coromandel Peninsula, New Zealand

N. Smith [a,*], J. Cassidy [a], C.A. Locke [a], J.L. Mauk [a], A.B. Christie [b]

[a] *Department of Geology, University of Auckland, Private Bag 92019, Auckland, New Zealand*
[b] *Institute of Geological and Nuclear Sciences, PO Box 31-312, Lower Hutt, New Zealand*

Received 2 December 2004; received in revised form 15 July 2005; accepted 18 September 2005

Abstract

Regional gravity data from an eroded Miocene to Pliocene volcanic arc exposed in the Coromandel Peninsula, New Zealand, delineate a circular −26-mGal, 15-km-diameter gravity anomaly. This anomaly, which has steep gradients on its northern and western margins but shallow gradients elsewhere, correlates with relatively young volcanic and volcaniclastic rocks within a broad topographic depression. Gravity modelling, using an exponentially decreasing density contrast with depth profile, requires very low-density rocks (ca. 2280 kg m^{-3}) in the near-surface to account for the observed anomaly, giving a total depth of ca. 2.8 km for these rocks. The northern and western margins of this body dip steeply inward at 70°, whereas the southern and eastern margins have shallow inward dips (20–30°). The western margin coincides with the regional-scale Mangakino Fault, but the northern margin, recognizable only in the geophysical data (and named here the Ohinemuri Fault), is partially buried under younger volcanic rocks. We interpret these deep and steeply bounded, low-density volcanics in terms of a trapdoor caldera, faulted on its northern and western margins, with its hinge on the southern and eastern margins. Epithermal deposits are spatially associated with the Mangakino and Ohinemuri Faults, suggesting that both structures may have influenced hydrothermal fluid flow. These deposits pre-date caldera fill, indicating that caldera development followed pre-existing regional faults. These results delineate the subsurface geometry of a trapdoor caldera and highlight the role of pre-existing, regional-scale faults in controlling such caldera location and collapse.

Keywords: trapdoor caldera; gravity model; volcanism; density; Waihi; Coromandel

1. Introduction

Reconstructing the relations between volcanic history, tectonism and fluid flow in the Earth's crust requires the recognition and delineation of large-scale volcanic features and structures. However, in regions of dense vegetation cover, few outcrops and extensive overburden, this can be problematic. Geophysical techniques, particularly gravity and magnetic methods, can be very effective for investigating structures in such volcanic terranes, particularly calderas (e.g., Cordell et al., 1985; Carle, 1988; Hallinan, 1993; Ferguson et al., 1994; McKee et al., 1999; Malengreau et al., 2000). The subsurface structural geometry of calderas, which is key evidence for their style of evolution, is often only apparent from geophysical data. Calderas enclosed by ring faults are common, but those that are bounded by polygonal faults are rare (Lipman, 1997). Active vol-

* Corresponding author. Fax: +64 9 373 7435.
E-mail address: n.smith@auckland.ac.nz (N. Smith).

0377-0273/$ - see front matter © 2005 Elsevier B.V. All rights reserved.
doi:10.1016/j.jvolgeores.2005.09.005

canic settings also commonly contain geothermal systems, which may form epithermal Au–Ag deposits (e.g., White, 1955; Henley and Ellis, 1983; Hedenquist and Lowenstern, 1994), localised by regional faults and calderas (e.g., Sibson, 1987; Sillitoe, 2000).

In this paper, we use new and existing gravity data to develop a model of a trapdoor caldera in the Waihi area of the Coromandel Peninsula, New Zealand. Trapdoor calderas result from asymmetrical collapse of caldera floors, resulting in steep-dipping margins on one side, and shallow-dipping margins on the other (Lipman, 1997; Cole et al., 2005). Several trapdoor calderas have been identified in the nearby Taupo Volcanic Zone (Wilson et al., 1984; Beresford and Cole, 2000; Milner et al., 2002), and similar structures occur worldwide (e.g., Rytuba and McKee, 1984; Seager and McCurry, 1988; Ferguson et al., 1994). Our gravity model allows the delineation of regional-scale faults and investigation of their role in controlling the location and nature of the Waihi caldera, as well as the possible relationship between these faults and former subaerial geothermal systems that formed epithermal Au–Ag deposits in the region.

2. Geological setting

2.1. Regional geology of the Coromandel Peninsula

The Coromandel Peninsula, located in North Island, New Zealand, is a Miocene to Quaternary volcanic province built on Mesozoic greywacke basement of the Manaia Hill Group (Skinner, 1972; Skinner, 1986). It is bounded to the west by the Hauraki Rift, a large graben filled with Quaternary and Tertiary sediments (Hochstein and Nixon, 1979; Hochstein and Ballance, 1993). To the south, the Coromandel Peninsula overlaps the presently active Taupo Volcanic Zone (TVZ). The Waihi area, which is the subject of the present study, is located at the southern end of the Coromandel Peninsula (Fig. 1).

The greywacke basement of the peninsula is divided into sub-rectangular fault blocks with NNW–SSE and WSW–ENE trends (Sporli, 1987; Gadsby and Sporli, 1989). These fault blocks are downthrown to the south, such that the volcanic cover becomes progressively thicker towards the southern end of the peninsula (Skinner, 1986). Volcanic activity began in the north at approximately 18 Ma and progressed gradually southward during the Miocene and Pliocene (Skinner, 1986; Adams et al., 1994). Early phases of volcanism were andesitic and dacitic in nature (Coromandel Group), with volcanism becoming more felsic with time (Whitianga Group), this trend continuing southward along the peninsula. Active volcanism in the Coromandel ended at approximately 1.5 Ma, at which time volcanism transferred to the TVZ without obvious breaks in activity (Adams et al., 1994; Carter et al., 2003).

A gravity study of the northern Coromandel Peninsula by Malengreau et al. (2000) revealed the presence of several large, circular negative anomalies, 10–25 km in diameter, with maximum anomalies of −26 to −34 mGal and gradients of about 2–3 mGal/km, which were attributed to calderas.

2.2. Geology of the Waihi area

In the Waihi area, the greywacke basement is thought to be directly overlain by units of the andesitic/dacitic Coromandel Group (Brathwaite and Christie, 1996), of which the two most important subgroups for this study are the Waiwawa (6.3–7.9 Ma) and Kaimai (3.5–5.6 Ma) (Fig. 1). The Waiwawa Subgroup chiefly crops out to the west and north of the Mangakino and Waihi faults, respectively, whereas the area to the east and south of these faults is dominated by the Uretara Formation of the Kaimai Subgroup. The Mangakino Fault marks a clear boundary between these units; however, the location of the contact along the Waihi Fault is obscured by sheets of younger ignimbrites of the Whitianga Group (Brathwaite and Christie, 1996). The Owharoa and Scotia faults have a similar orientation to the Mangakino Fault and align approximately with its northern extrapolation, forming a structural corridor of N–NNE-trending faults (Brathwaite and Christie, 1996).

Several large epithermal mineral deposits occur in the Waihi area, the largest of which are the Au–Ag deposits at Waihi (Martha), Karangahake and Golden Cross, the Zn–Pb–Cu deposit at Tui (Brathwaite et al., 1989), and the newly defined Favona Au–Ag deposit (Simpson et al., 2002) (Fig. 1). Together, these deposits have produced over 85% of the Au–Ag bullion from the Hauraki Goldfields (Brathwaite and Pirajno, 1993). They are chiefly hosted in the Waipupu Formation andesites of the Waiwawa Subgroup and are associated with extensive areas of hydrothermal alteration (Brathwaite and Christie, 1996). There is little evidence of hydrothermal alteration in the younger Omahine and Kaimai subgroups, and no significant epithermal deposits have been found in these units (Brathwaite and Christie, 1996). Thus, the largest (Martha, Waihi) and third largest (Karangahake) epithermal Au–Ag deposits in the Hauraki Goldfields, as well as several other

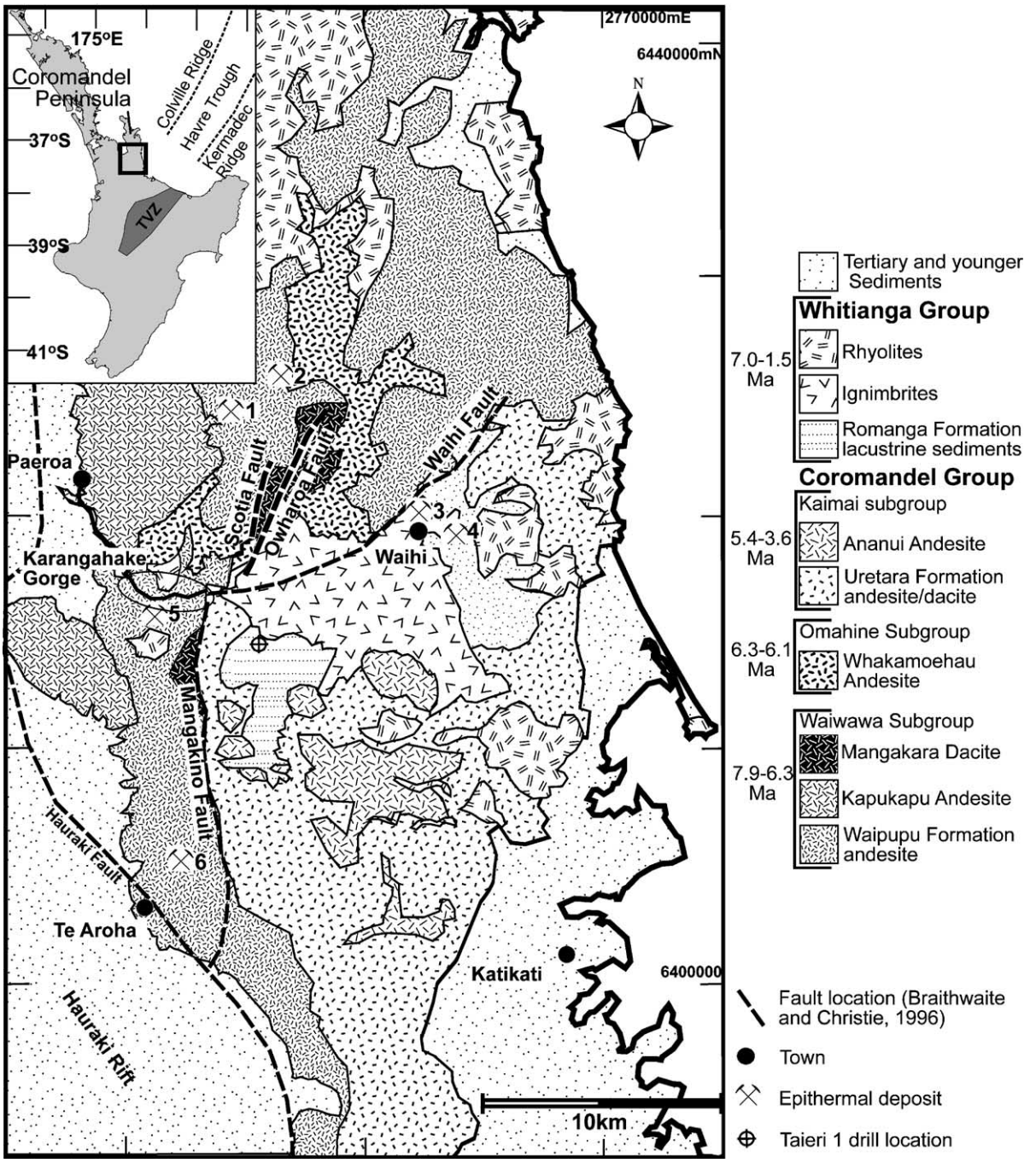

Fig. 1. Simplified geology of the Waihi region, southern Coromandel Peninsula (from Brathwaite and Christie, 1996), and locations of epithermal deposits. (1) Komata, (2) Golden Cross, (3) Martha Hill, (4) Favona, (5) Karangahake, (6) Tui. The locations of the Waihi and Mangakino faults are shown. Inset: Location map showing North Island, New Zealand. Boxed region of Coromandel Peninsula is the Waihi Region. Also shown are the Colville and Kermadec Arcs, the Havre Trough back-arc basin, and the Taupo Volcanic Zone (TVZ).

epithermal mineral deposits, occur within 5 km of the Waihi or Mangakino/Owharoa/Scotia Fault systems.

Regional gravity data reveal the presence of a large negative gravity anomaly to the south of Waihi (Woodward, 1971) that is of similar magnitude to those in the northern Coromandel, though it differs in being asymmetrical in form. It is bounded to the north and west by steep, linear gravity gradients that

intersect orthogonally, whereas the southern and eastern margins, though poorly defined, have much shallower gradients. This gravity anomaly has previously been attributed to either a caldera, a fault-angle depression, or some combination of the two (Bromley and Brathwaite, 1991; Brathwaite and Christie, 1996); however, the regional gravity data were too sparse to resolve the details of this structure (known as the Waihi Basin).

Of possible significance, also, is the occurrence of a major magnetic anomaly centred 7 km southeast of the Waihi gravity anomaly, which may represent a buried intrusion at depth (Couper and Lawton, 1978; Stagpoole et al., 2001). Several workers have identified links between calderas, hydrothermal systems and epithermal deposits (Sillitoe, 1993, 2000; Hedenquist and Gakkai, 1996; Guillou et al., 2000). If the Waihi Basin is a caldera, it may have important implications for understanding the development of these hydrothermal systems.

3. Gravity data acquisition and processing

3.1. Gravity survey

A total of 130 new gravity measurements have been collected in the Waihi area using a La Coste and Romburg G Meter. Height control for the gravity stations through differential global positioning system (DGPS) to an accuracy of ± 15 cm is tied to bases of known heights (m a.s.l.). The gravity data are tied to the New Zealand Potsdam 1959 system (Robertson and Reilly, 1960) through four stations of the Precise Gravity Network and have been corrected using a density of 2670 kg m^{-3} (Reilly, 1972). Terrain corrections to a distance of 22.9 km have been applied to each gravity measurement. The total estimated error in the corrected gravity data is ± 0.1 mGal and is mainly due to uncertainty in the terrain corrections. These data have been combined with existing data (Woodward, 1971; Reilly, 1972) to give the absolute Bouguer anomaly map (Fig. 2), which clearly defines a negative gravity anomaly to the south of Waihi, bounded to the north and west by linear gravity gradients.

3.2. Regional gravity field and residual anomaly map

The regional gravity field in the Waihi area has been approximated by a third-order polynomial surface fitted to the gravity data collected on the least altered Coromandel Group andesites (Fig. 2). This regional field has been subtracted from the observed Bouguer gravity anomaly data to give the residual gravity anomaly (Fig. 3).

The residual gravity anomaly map (Fig. 3) is dominated by an approximately circular -26 mGal anomaly, 15 km in diameter and centred south of Waihi. This anomaly is of similar dimensions and magnitude as those further north in the Coromandel Peninsula which have been attributed to filled calderas (Malengreau et al., 2000). The steep (5 mGal km^{-1}) gravity gradients on the northern and western margins of the anomaly correlate with the mapped locations of the Mangakino Fault and western end of the Waihi Fault (Fig. 3) (Brathwaite and Christie, 1996). The mapped intersection of these two faults coincides with a general change in the trend of the gravity gradient from N–S to E–W (Fig. 3). The eastern continuation of the Waihi Fault, however, trends NE (Fig. 3), whereas the gravity gradient continues due east to the south of Waihi, before broadening and trending southeast. The eastern and southern margins of the gravity anomaly are characterised by shallower gradients (2–3 mGal km^{-1}). The steep (4–5 mGal km^{-1}) west-dipping gradient, located on the far western side of the survey area, results from the down-faulted western boundary of the Coromandel Peninsula and Hauraki Rift (Hochstein and Nixon, 1979; Hochstein and Ballance, 1993).

4. Rock densities and gravity modelling

4.1. Rock densities

Laboratory density measurements of field samples of least altered Waipupu Formation andesite gave densities of 2640–2690 kg m^{-3} (mean 2670 kg m^{-3}). These density values agree with other samples of Waipupu andesites from both surface and subsurface samples (M. Simpson, personal communication, 2003), and drill hole density data from the Waihi deposit (unpublished data, Newmont Waihi Ltd.) (Table 1).

The Uretara Formation contains a range of lithologies, including lavas, tuffs, breccias and some sedimentary units (Brathwaite and Christie, 1996), and most outcrops are weathered. Hence, the bulk density is difficult to estimate, and therefore, an analytical approach to density determination is taken. An estimate of the average proportions of component lithologies in the Uretara Formation can be obtained from engineering logs of the Kaimai railway tunnel, which passes through a 1.4-km stratigraphic thickness of Uretara Formation 13 km to the south of the study area (Hegan, 2003). The 9-km-long tunnel section consists

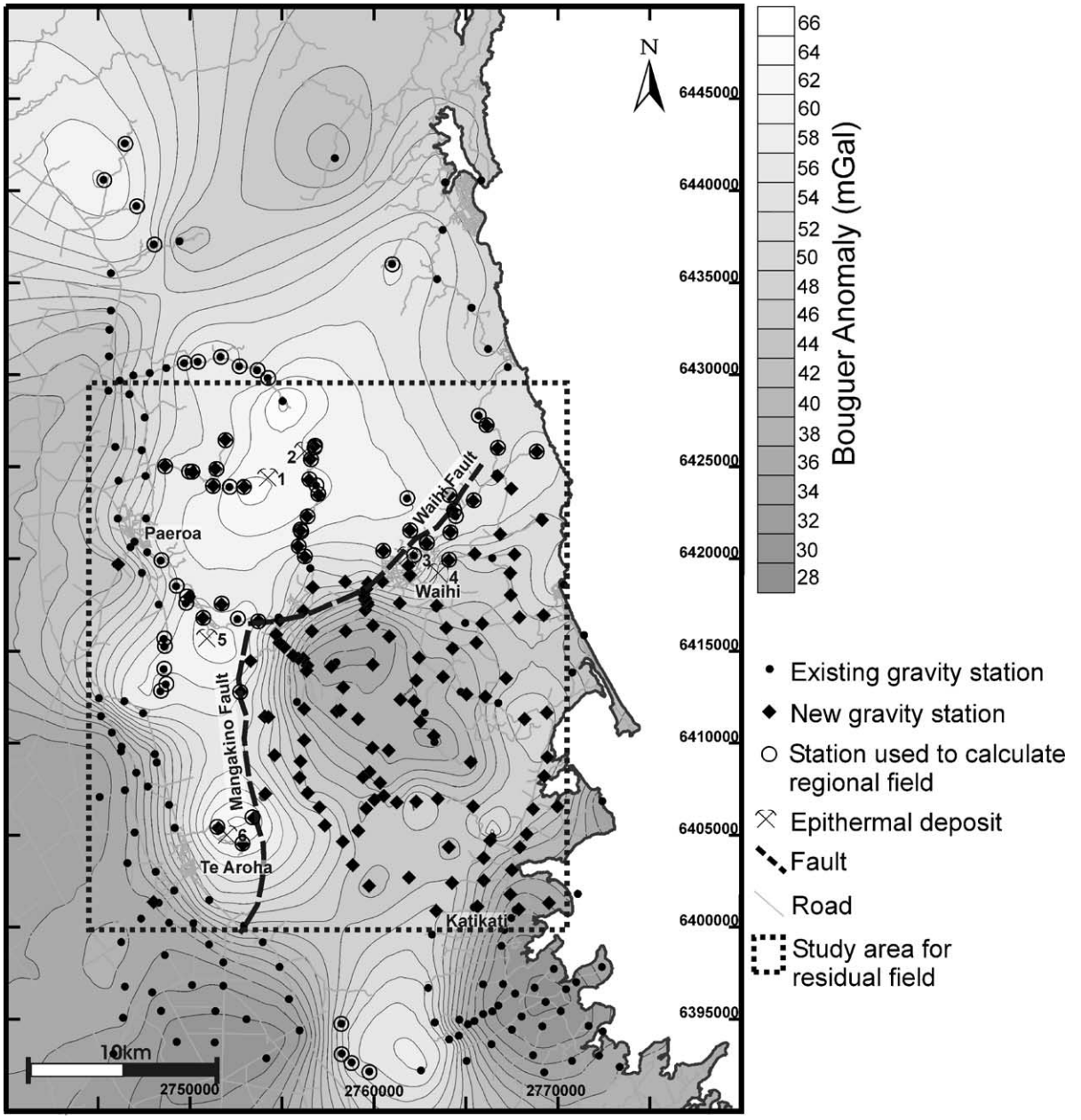

Fig. 2. Absolute Bouguer anomaly map of the Waihi region, showing gravity station locations from this study and existing gravity data (Woodward, 1971). For details of faults and epithermal deposits, see Fig. 1. Stations used for determination of regional field (i.e., located on Coromandel Group andesites) are shown circled. Outlined area shows the limits of the residual gravity anomaly map (Fig. 3).

of andesite flows (45%), altered andesite (8%), breccias (25%), tuff (20%) and sediments (2%). Published densities for these rock types are andesite (2670 kg m^{-3}), altered andesite (2400 kg m^{-3}), breccia (1900 to 2400 kg m^{-3}), tuff (1900 to 2200 kg m^{-3}) and sediments (1900–2100 kg m^{-3}) (Hatherton and Leopard, 1964; Hoover et al., 1992), hence giving an estimated near-surface bulk density range of 2280–2460 kg m^{-3}.

4.2. Rate of increase of density with depth in the Waihi Basin fill

Although the stratigraphy of the basin fill is unknown, the surface is dominated by Uretara Formation. Brathwaite and Christie (1996) interpreted this unit as continuous to depths greater than 1 km, directly overlying the Waiwawa Subgroup andesite basement. For

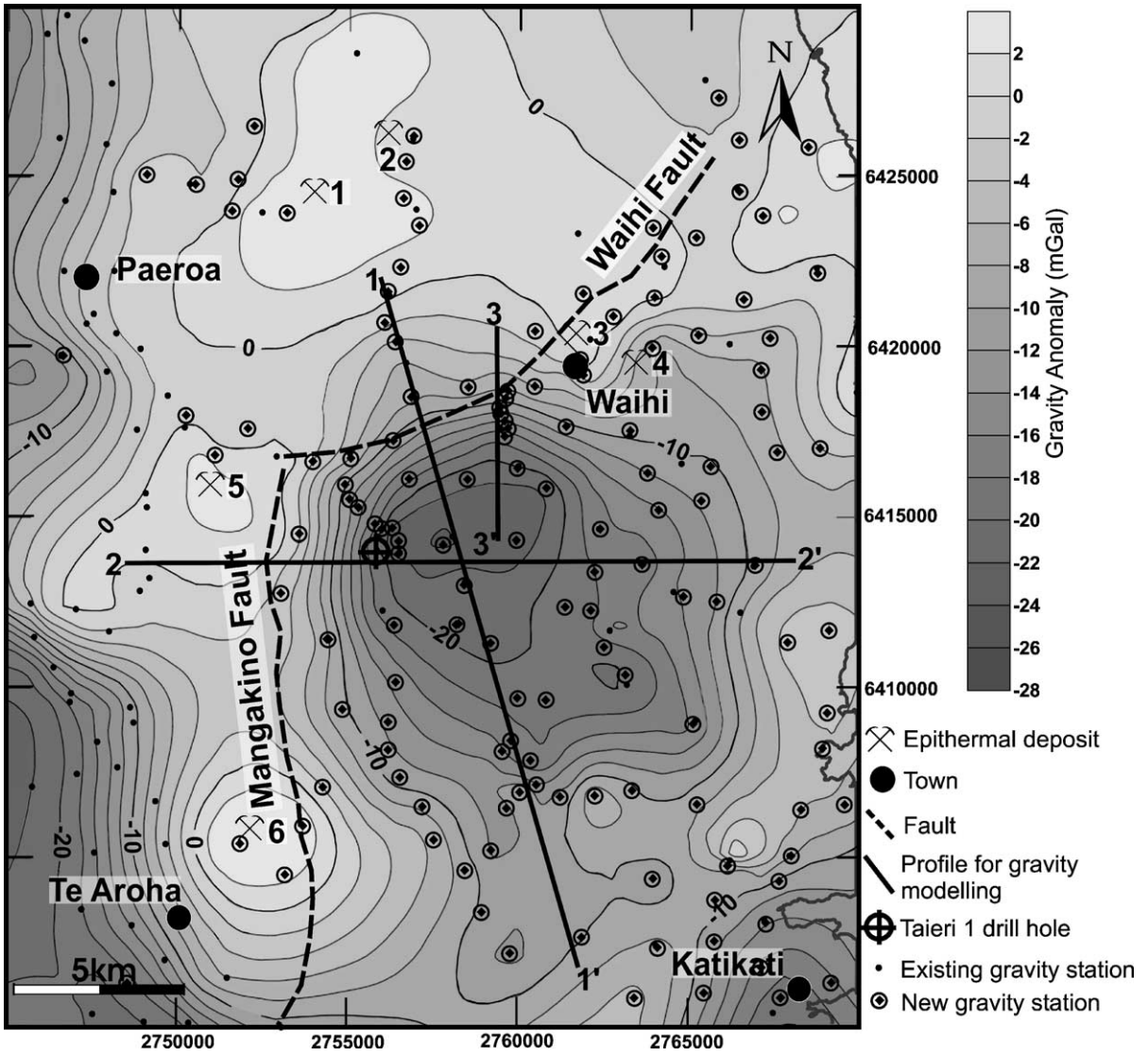

Fig. 3. Residual gravity anomaly in the study area. New and existing gravity station locations are shown, as is the position of the Taieri 1 drill hole, located near the profile intersections. For details of faults and epithermal deposits, see Fig. 1. Profiles for gravity modelling are shown (1–1′, 2–2′, 3–3′).

the purposes of determining density, therefore, it is assumed that the basin fill is compositionally similar to the Uretara Formation observed in the Kaimai Railway tunnel. Given the large proportion of breccia and tuff in the basin fill, it is likely that its density will increase with depth due to lithostatic pressure. Although data on the rate of density increase with depth for volcanic rocks is sparse, studies of geothermal fields in the TVZ report density increases in volcanic rocks from 1800 to 2100 kg m^{-3} at the surface to 2650 kg m^{-3} at a depth of approximately 3 km, with the rate of density increase decreasing exponentially with depth (Stern, 1982; Soengkono, 1985). These rocks in the TVZ are composed of andesite, dacite, ignimbrite, rhyolite, breccia, tuff and some sedimentary sandstone (Stern, 1982). Although the Uretara Formation contains similar rock types, the proportion of andesite is much larger and, therefore, has a higher near-surface density. Thus, for the basin fill, an exponential rate of decreasing density contrast with depth was also assumed, i.e.,

$$\Delta\rho = \Delta\rho_0 \exp(-\beta z)$$

where $\Delta\rho$ = density contrast, $\Delta\rho_0$ = density contrast at the surface ($z=0$), z = depth, and β is a variable from 0.3 to 1.5 which represents the compressibility of the rocks (Cordell, 1973).

Table 1
Density of Waipupu formation andesites

Waipupu Formation andesite	Source	Density range (kg m^{-3})	Number of samples	Average value (kg m^{-3})
Unaltered	Field samples	2640–2690	8	2670
Altered/unaltered (least altered)	Drill hole and other sources (M. Simpson, personal communication, 2003)	2010–2750 (2670)	86 (1)	2500 (2670)
Altered/unaltered (least altered)	Newmont Waihi drill hole data	2070–2710 (2640–2710)	241 (7)	2490 (2660)

Data for this study come from field samples and drill hole data. Drill hole data contain both altered and unaltered samples. Least altered samples are shown in parentheses.

The maximum density at depth will be that of the Waipupu andesite (2670 kg m^{-3}), whereas both β and $\Delta\rho_0$ are less well constrained. Stern (1982) reported β values of 0.83–0.87 for the Wairekai and Kawerau geothermal fields and ρ_0 values of 1810 kg m^{-3} and 2090 kg m^{-3} respectively, reflecting the small proportion of andesite (1–2%). However, the Uretara Formation consists of approximately 50% andesite and is therefore much less compressible, making a lower value for β appropriate. Since a β value of 0.3 represents essentially incompressible rocks, a median β value of 0.55 was assumed. A density-vs.-depth graph using a β value of 0.55 and values from the measured range of ρ_0 for the basin fill, together with data from the Wairekai and Kawerau geothermal fields, is shown in Fig. 4. This graph shows the curves of low-density rocks with high values of β, and higher density rocks with lower β, converge at depth as their density approaches 2670 kg m^{-3}. Obviously, near-surface rocks, which have the greatest density contrast, are the most significant contributor to the gravity anomaly. Determination of the near-surface density is therefore critical to accurately constrain the thickness of the body causing the gravity anomaly.

4.3. Modelling constraints

Gravity models (developed using Interpex Magix XL, V3) were constrained by surface geology (Brathwaite and Christie, 1996) and a single drill hole, Taieri 1, located close to the centre of the anomaly (Fig. 3), which penetrated to a depth of 190 m (Rabone,

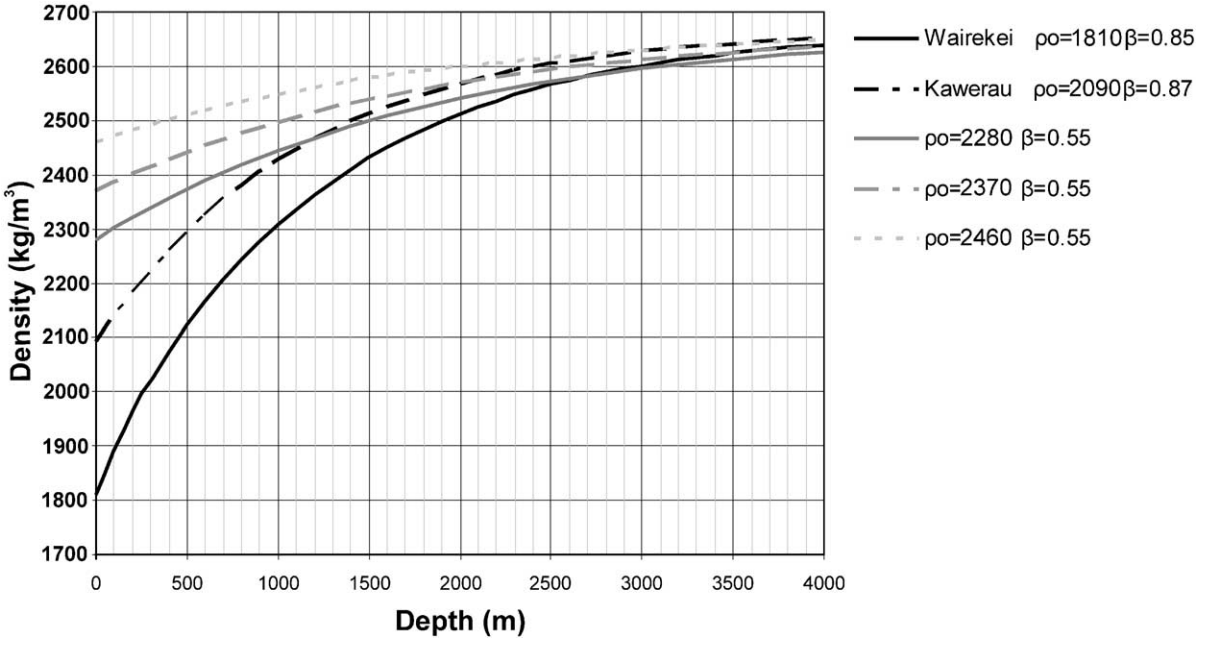

Fig. 4. Comparison of density increase with depth curves for data from the Wairakei and Kawerau geothermal fields (Stern, 1982) and data from this study based on varying near-surface density from 2280 to 2460 kg m^{-3} and β of 0.55. The data show that all curves approach a density of 2650 kg m^{-3} by 3 km depth.

1987). This drill hole gives a local depth limit of 150 m for sediments of the Romanga Formation, below which Uretara Formation occurs. Ten kilometres north of this drill hole, the Romanga Formation is up to 160 m thick (Brathwaite and Christie, 1996). In addition, resistivity surveys suggest that the Romanga Formation may reach thicknesses of several hundred meters to the south of the Waihi Fault (Bromley and Brathwaite, 1991).

Gravity models were developed along three profiles across the Waihi gravity anomaly (Fig. 3), two of which are oriented perpendicular to the gravity gradients which define the margins of the gravity anomaly and pass through the maximum anomaly, with N–S and E–W orientations. The third profile is oriented N–S and is located to investigate the projected trend of the Waihi Fault near Waihi (Fig. 3). The gravity modelling was carried out in 2.75D (i.e., uneven half-widths could be used as appropriate for the component bodies). The 2.75D models along each profile were constructed to ensure consistency through an equivalent and coherent 3D model. The geometry of the models was constrained by the known geology and was varied iteratively to achieve an optimal fit, determined by the root mean square (RMS) discrepancy between the calculated gravity effect and the observed gravity data. For each model, once an optimal fit was approached manually, the fit was optimised automatically by the programme through adjustment of the model geometry. The uncertainties in the location and dip of the main boundaries of the models were estimated by determining the limits of each parameter beyond which the RMS discrepancy between the calculated and observed gravity values significantly increased.

The relationship of the cumulative gravity effect to total thickness of basin fill, for a range of ρ_0 values and a β value of 0.55 (Fig. 5), shows that the observed anomaly cannot be reasonably accounted for if ρ_0 exceeds the maximum or median estimates of near-surface density, as these result in a basin much deeper than 8 km. Hence, the maximum thickness of basin fill cannot be resolved; however, a minimum thickness of approximately 2800 m can be defined by using the minimum ρ_0 value of 2280 kg m^{-3}. For the purposes of modelling, the basin fill has been divided into a series of layers, the densities of which are summarised in Table 2, which also shows the effect of altering β by ± 0.05.

4.4. Profile 1

The N–S gravity profile (Fig. 6) shows gravity rapidly decreasing from the north, to a minimum of -25 mGal. To the south of this minimum, gravity increases gradually to -8 mGal. The model comprises an asymmetric wedge of lower density rocks, with a steep northern boundary and shallow dipping southern boundary, filling a depression in the down-dropped Waipupu Formation. For the steep northern boundary,

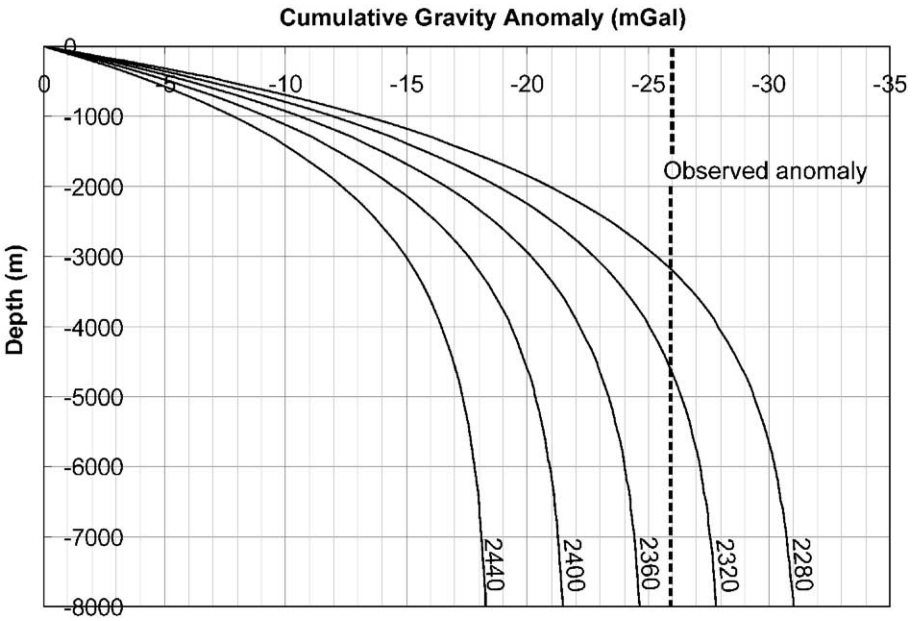

Fig. 5. Plot of the cumulative gravity effect, for varying near-surface densities, of a Bouguer slab given a β of 0.55. Curve labels indicate near-surface density. The plot shows the maximum value of the observed Waihi gravity anomaly.

Table 2
Density values for 200 m thick layers of basin fill, given a starting density of 2280 kg m^{-3} and a β value of 0.55

Depth to top of layer (m)	β = 0.60		β = 0.55		β = 0.50	
	Cumulative gravity anomaly (mGal)	Density of layer (kg m^{-3})	Cumulative gravity anomaly (mGal)	Density of layer (kg m^{-3})	Cumulative gravity anomaly (mGal)	Density of layer (kg m^{-3})
–2000	–21.19	2553	–22.02	2540	–22.92	2527
–2200	–22.06	2566	–22.98	2554	–24.00	2540
–2400	–22.83	2578	–23.87	2566	–24.99	2553
–2600	–23.52	2588	–24.65	2577	–25.88	2564
–2800	–24.13	2597	–25.35	2586	–26.69	2574
–3000	–24.67	2606	–25.98	2595	–27.42	2583
–3200	–25.15	2613	–26.54	2603	–28.08	2591
–3400	–25.57	2619	–27.05	2610	–28.67	2599
–3600	–25.95	2625	–27.50	2616	–29.21	2606
–3800	–26.29	2630	–27.90	2622	–29.70	2612
–4000	–26.58	2635	–28.26	2627	–30.14	2617

Highlighted values are those which approach the observed maximum gravity anomaly.

a best-fit was achieved with a 70°(± 10°) south-dipping boundary approximately 2600 m in vertical extent which is coincident with and thus interpreted as the Waihi Fault, across which higher density Waipupu Formation is faulted against the lower density basin fill. The exact nature of the upper portion of the

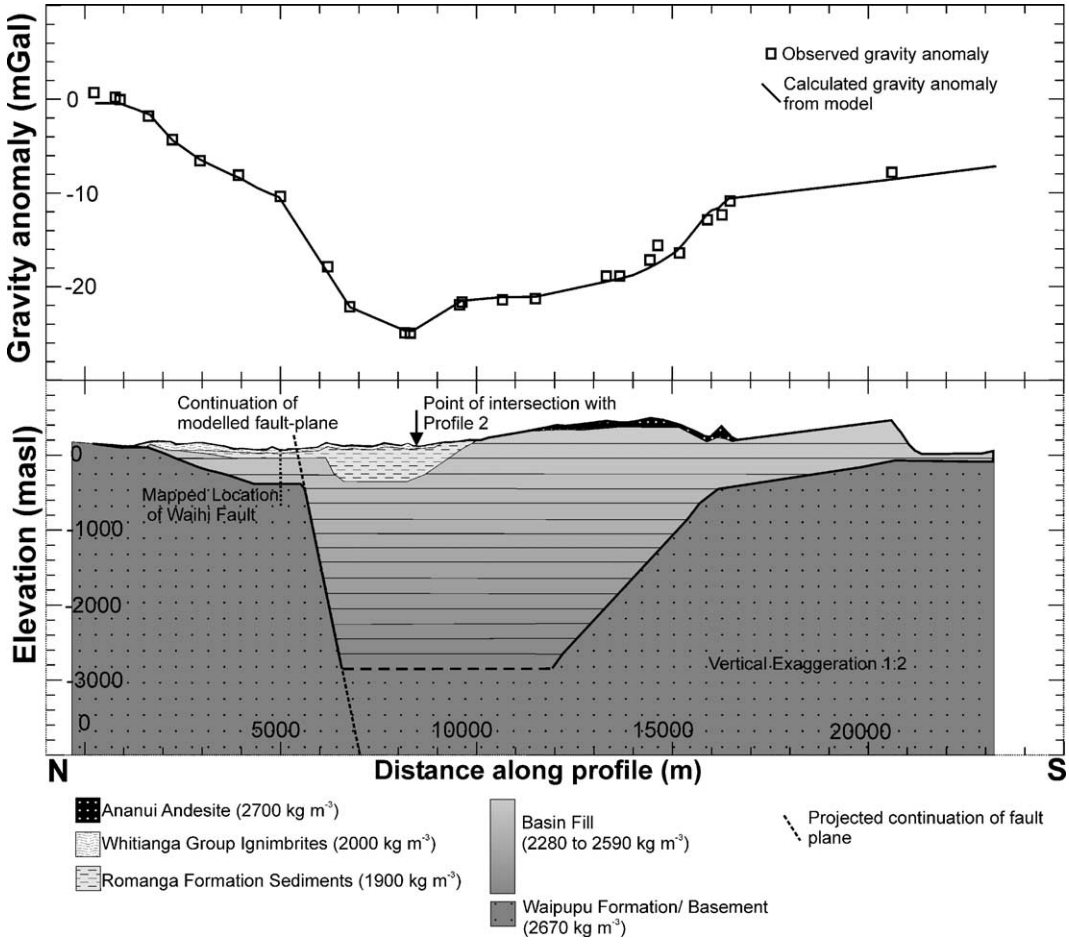

Fig. 6. Profile 1 (location shown in Fig. 3). Diagram shows observed and calculated gravity data and 2.75D profile model. Unit densities are shown in brackets. Densities for layers of the basin fill can be found in Table 2. Density values for other units are from field samples or published densities (Hatherton and Leopard, 1964; Whitford and Lumb, 1975; Hoover et al., 1992).

Waihi Fault has a measure of uncertainty due to the proximity of the 400-m-thick unit of Romanga Formation sediments.

South of the fault boundary, the Waipupu Formation is modelled at a depth of 2800 m before gradually shallowing to the south at 30°(± 10°) dip. This total thickness of basin fill is a minimum because the increase in density with depth results in very little density contrast between the fill and Waipupu Formation andesite at depth. Near the profile centre, an outcrop of Ananui Andesite occurs which has previously been interpreted as the top of a substantial buried dome (Brathwaite and Christie, 1996). Such an interpretation is not supported by the observed gravity data, since a large dome of this material (density 2700 kg m^{-3}) would be expected to result in an observable anomaly, whereas the observed gravity data can be accounted for by a 200–300 m thick series of andesite flows. The RMS discrepancy between the calculated gravity effect and the observed anomaly for the optimum model is 0.7 mGal, i.e., 2.5% of the maximum observed anomaly.

4.5. Profile 2

Profile 2 (Fig. 7) is oriented W–E and crosses the Mangakino Fault 3 km south of the intersection with the Waihi Fault and intersects Profile 1 near the maximum gravity anomaly. The gravity profile shows a rapid decrease from the west, to a minimum of −25 mGal, followed by a gradual increase to the east. Similar to Profile 1, an asymmetric wedge of lower density rock, with a steep western boundary and shallow-dipping eastern boundary, filling a depression in the down-dropped Waipupu Formation is required to account for the observed gravity anomaly. The western boundary has been modelled as a 60° (± 10°) dipping boundary

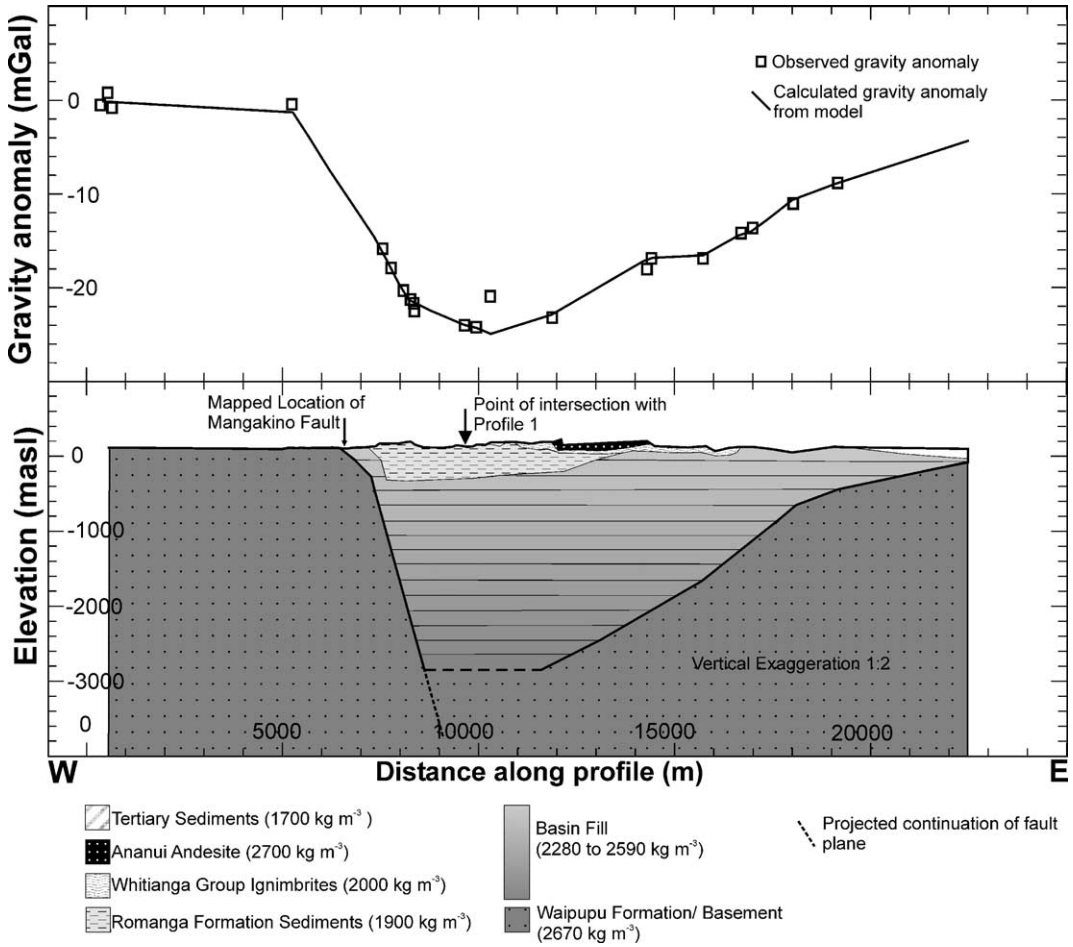

Fig. 7. Profile 2 (location shown in Fig. 3). Diagram shows observed and calculated gravity data and 2.75D profile model. Unit densities are shown in brackets. Densities for layers of the basin fill can be found in Table 2. Density values for other units are from field samples or published densities (Hatherton and Leopard, 1964; Whitford and Lumb, 1975; Hoover et al., 1992).

of 2600 m vertical extent between the higher density Waipupu and lower density basin fill, co-incident with the known location of the N–S-striking Mangakino Fault. This profile varies from profile 1 in that the Waipupu Formation floor continues at 2800 m depth for only 2.5 km before it begins to rise with a smooth 15–20° west-dipping gradient.

The profile crosses an exposed body of Ananui Andesite near the profile centre, and as with profile 1, modelling this unit as a 200-m-thick sheet provides a close fit to the observed data. To the east of this andesite body, the profile crosses an exposed body of Whitianga Group Corbett Ignimbrite. Drill core samples from nearby sites have shown this ignimbrite layer to be approximately 50 m thick, overlying a 20-m thickness of Romanga Formation that overlies either Uretara Formation or Homunga Rhyolite in various locations (Brathwaite and Christie, 1996). A 50–100-m-thick unit of ignimbrite provides a close fit to the observed gravity. The RMS discrepancy between the calculated gravity effect and the observed anomaly for the optimum model is 1.3 mGal, i.e., 5% of the maximum observed anomaly.

4.6. Profile 3

Profile 3 (Fig. 8) is oriented N–S and crosses the E–W-oriented gravity gradient and the mapped location of the Waihi Fault. The observed gravity anomaly shows a strong decrease to the south to a minimum of −25 mGal. The Waihi Fault has been previously mapped in this area with a NE strike (Brathwaite and Christie,

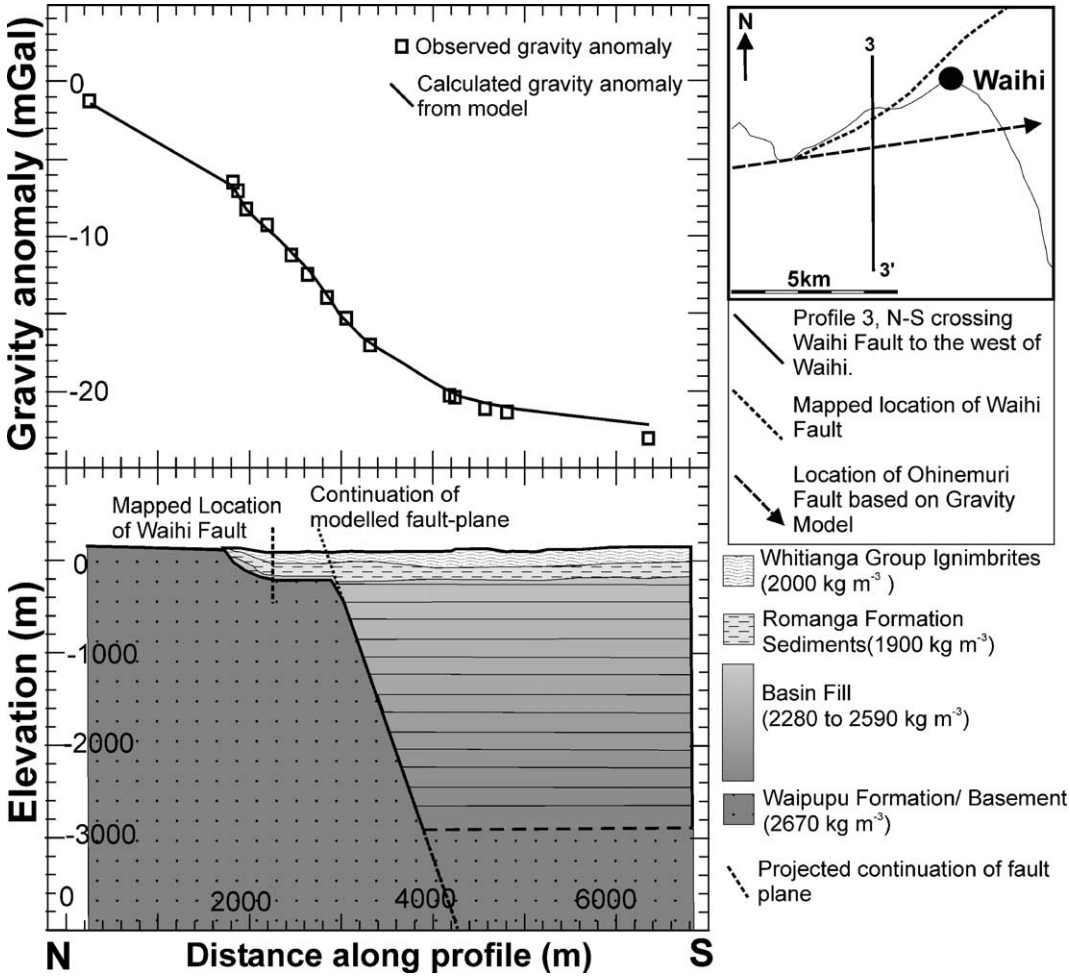

Fig. 8. Profile 3 (location shown in Fig. 3). Diagram shows observed and calculated gravity data and 2.75D profile model. Unit densities are shown in brackets. Densities for layers of the basin fill can be found in Table 2. Density values for other units are from field samples or published densities (Hatherton and Leopard, 1964; Whitford and Lumb, 1975; Hoover et al., 1992). Inset shows a section from the regional geology map (Brathwaite and Christie, 1996) showing the mapped location of the Waihi Fault, profile location and interpreted position of the Ohinemuri Fault projected from the gravity model.

1996); however, the gravity gradients that define the northern margin of the Waihi gravity anomaly trend E–W and are located to the south of the mapped fault location. Only a very shallow gravity gradient is observed at the mapped fault location, and the observed gravity anomaly at this point is almost zero, suggesting that the Waipupu Formation is at very shallow depth.

Gravity modelling shows that the major density contrast at depth, i.e., the fault contact, must be located approximately 800 m south of the mapped fault location. The mapped gravity gradients suggest the divergence between the modelled and mapped fault location increases to the east. This fault is modelled as a steeply south-dipping 70°(± 10°) boundary of 2600 m vertical displacement, similar to that modelled in profile 1. This location is consistent with an extrapolation of the known E–W strike of the western end of the Waihi Fault. We suggest this E–W-striking fault from the eastern end of the Karangahake Gorge, and passing south of Waihi, be named the Ohinemuri Fault to differentiate it from the Waihi Fault which strikes NE, passing to the north of Waihi (Fig. 8). The RMS discrepancy between the calculated gravity effect and the observed anomaly for the optimum model along this profile is 0.3 mGal, i.e., 1.5% of the maximum observed anomaly.

4.7. Discussion of modelling

Gravity modelling shows that the negative gravity anomaly south of Waihi can be accounted for by an asymmetrical depression above the Waipupu Formation, filled with at least 2.8 km of less dense material. The western and northern margins of this structure, the Waihi Basin, are modelled as 60° and 70°(± 10°) boundaries with 2600 m vertical displacement, which correlate with the Mangakino and Ohinemuri Faults respectively. The southern and eastern boundaries of the basin dip at 20–30°. Although the northern and western faulted margins have been modelled as single planes, they may actually be a series of stepped faults. Similarly, the southern and eastern margins have been modelled as smoothly dipping planes, but they may be a series of broad step faults. Since the gravity gradient associated with each step would be small, such stepped faults would not be resolved with the gravity method. A similar gravity-based study on the asymmetric Guayabo caldera, Costa Rica (Hallinan, 1993) did identify several sets of small concentric ring faults (rather than a single major ring fault); however, data from extensive drilling were available to provide geological control on detailed gravity modelling.

The density profile through the low-density Waihi Basin fill has been deduced by assuming a β value of 0.55. An error of ± 0.05 in this value would result in a range of minimum depths between 2400 and 3200 m; thus, the error on the model depth due to β is estimated to be ± 15%. A minimum β value of 0.3, though unrealistic, would result in a minimum depth of 2000 m, whereas increasing β by only 0.15 results in an unreasonable depth of greater than 8 km. There may be some further uncertainty on the modelled dips of the boundary faults if large volumes of lower density slumped material occur near these margins, as has been proposed near the steep margins of calderas (Lipman, 1997).

5. Interpretation of results

5.1. The Ohinemuri and Mangakino faults

Modelling of profile 3 shows that the Ohinemuri Fault is an E–W-trending structure, which follows the steep gravity gradient south of the Waihi and Favona epithermal deposits. This result is consistent with the fact that both these deposits are hosted in shallow Waipupu Formation. Displacement along the Mangakino Fault north of the Ohinemuri Fault or along the Ohinemuri Fault west of the Mangakino Fault cannot be determined from either geological mapping or gravity data, due to a lack of density contrast. Faulting on the scale seen in the Waihi Basin would result in the down-dropping of the Waipupu Formation andesite and would either result in an extensive fault scarp or deposition of contrasting covering rocks. As neither of these is evident, if there is offset, it is likely to be on a smaller scale than to the southeast.

The continuation of the Ohinemuri Fault to the east follows the same orientation as the sub-rectangular regional faults that have been observed in the northern Coromandel, and which has influenced the orientation of faults in the overlying Tertiary rocks (Skinner, 1986; Sporli, 1987). A recent structural study of the Karangahake Gorge (Fig. 1) identified possible E–W shear structures (Smith, 2003), which suggests a westward continuation of the Ohinemuri Fault. The north and west boundary faults of the basin may therefore represent major pre-existing crustal-scale faults which have been reactivated in the Miocene to Pliocene.

5.2. Tectonic setting of the Waihi Basin

Calderas in the TVZ occur in a zone of regional extension and crustal thinning with a NE–SW structural

trend (Davey et al., 1995; Wilson et al., 1995; Ballance et al., 1999), and a similar structural trend has been observed in the southern Coromandel (Bromley and Brathwaite, 1991). Present-day crustal extension in the TVZ has resulted in extension of up to 80% (Davey et al., 1995), and crustal thicknesses of 15 km are observed in the TVZ (Stern and Davey, 1987; Bibby et al., 1995), compared to crustal thicknesses away from the plate boundary of 25–28 km (Stern, 1985). This anomalously thin crust has led to higher heat flow and voluminous andesitic, dacitic and rhyolitic eruptions (Wilson et al., 1984, 1995). The Waihi area is the volcanic precursor to the adjacent TVZ, related to the same subduction system, and thus, the observed NE–SW trend of faults in the Waihi area may be the result of a similar NW–SE extension in the late Miocene and early Pliocene.

Evidence for Miocene/Pliocene NW–SE extension in the Coromandel can be found in the Kermadec arc system, related to the subduction of the Pacific Plate beneath the Australian Plate. The arc system is comprised of the parallel Colville and Kermadec ridges, separated by the Havre trough, which is interpreted to be a back-arc basin (Ballance et al., 1999). Whereas the Kermadec Ridge is the active offshore continuation of the of the TVZ (Adams et al., 1994; Ballance et al., 1999), projection of the trend of the Colville Ridge intercepts the southern Coromandel Peninsula near Waihi. NW–SE extension of the Havre Trough is thought to have initiated at approximately 5 Ma (Wright, 1993), but the exact timing remains uncertain (Ballance et al., 1999).

Dredge samples from the Colville Ridge showed that there was volcanic activity along the ridge at and before 5.4 Ma (Adams et al., 1994), and marine tephras record phases of rhyolitic volcanism in the Coromandel in the Miocene, from 7.7 to 7.0, and 6.3 to 4.0 Ma (Carter et al., 2003). This second phase records an extremely large rhyolitic eruption at 6.3 Ma and included a large cluster of eruptions occurring at around 5.2 Ma (Carter et al., 2003). The Uretara Formation has been determined as approximately 5.6–4.3 Ma, and several rhyolites in the Waihi area date from 7 to 5 Ma (Brathwaite and Christie, 1996). Thus, it appears that at around 6–5 Ma, there was a marked increase of rhyolitic and andesitic volcanism in the southern Coromandel, just prior to a shift in the active arc location from the Colville to the Kermadec Ridge, and the onset of spreading in the Havre Trough.

5.3. The Waihi Basin as a trapdoor caldera

A characteristic of calderas is that they typically contain large volumes of ignimbrites and breccias (Lipman, 1997; Cole et al., 2005). Calderas in the northern Coromandel have similar physical sizes and depths (up to 2 km) as the Waihi Basin and are filled with low-density rhyolitic and ignimbritic deposits (Malengreau et al., 2000). The modelled near-surface density of 2280 kg m^{-3} for the Waihi structure strongly suggests that the fill may be of lower average density than would be expected if it consisted solely of Uretara Formation (as estimated from the Kaimai tunnel transect). Thus, the fill material at Waihi is also likely to include a significant proportion of lower density, rhyolitic rocks at depth. Although we have no evidence, apart from gravity modelling, for rhyolitic rocks above the Waipupu Formation and beneath the Uretara Formation within the Waihi Basin, there are many examples of rhyolitc rocks pre-dating the Uretara Formation in the Waihi area. These include Maratoto Rhyolite and Rahu Formation (rhyolitic tuff), with an estimated age of 7–6 Ma, to the west of the Waihi Basin, and, in the eastern side of the basin, a large body of Homunga Rhyolite, K–Ar dated at 5.5–5.1 Ma, that overlies, and is intercalated with Uretara Formation (Brathwaite and Christie, 1996). Therefore, rhyolitic volcanism occurred in the region before deposition of the Uretara Formation, and we interpret the modelled depression as a caldera, partially filled with low-density rhyolitic rocks that are masked by a thick overlying unit of Uretara Formation. Depending on the volume of low-density rhyolitic material at depth, caldera depth may be less than modelled; however, lower density rocks have a higher β value, and thus, the resulting change in depth is likely to be small.

In many trapdoor calderas, collapse is controlled by a pre-existing structural fabric (Lipman, 1997; Cole et al., 2005). In the case of the Waihi Basin, the Ohinemuri and Mangakino Faults may have provided structural weaknesses in the crust which acted to localise a caldera forming eruption (Cole et al., 2005). The resulting caldera collapse resulted in a polygonal-shaped trapdoor caldera, with the fault planes forming the steep northern and western margins. Collapse in the southern and eastern sectors of the caldera was less and resulted in the observed shallow-dipping eastern and southern margins.

Ignimbrite units interpreted as intra-caldera are restricted to the area of the Waihi Basin (Brathwaite and Christie, 1996), and the stratigraphy shows that they overlie the Uretara Formation and Romanga Formation sediments. The three recognized ignimbrite units, the Corbett, Owharoa, and Waikino have K/Ar ages of approximately 3, 2.6 and 1.5 Ma, respectively (Brathwaite and Christie, 1996). The presence of the

sedimentary units of the Romanga Formation suggests that a depression existed prior to the deposition of these ignimbrite units, and they represent a later eruption of volcanic material from a local source. Most pre-Holocene calderas are completely filled with a variety of material including sediments, volcanic material from separate volcanic centres and younger lavas and tuffs erupted from post-collapse caldera-related vents (Lipman, 1997), and it may be that these ignimbrites represent a stage of post-collapse volcanism within a caldera structure.

Interpretation of the Waihi Basin as a caldera implies the presence of a shallow magma body during formation, but there is no direct evidence for such a body in either the surface geology or gravity data. The gravity effect of such a body, however, may be small and, therefore, masked by the strong negative anomaly caused by the caldera fill. Regional aeromagnetic maps do reveal the presence of a large 12-km-diameter 800-nT anomaly, but centred 7 km southeast of the centre of the Waihi gravity anomaly (Couper and Lawton, 1978; Stagpoole et al., 2001) (Fig. 9). Couper and

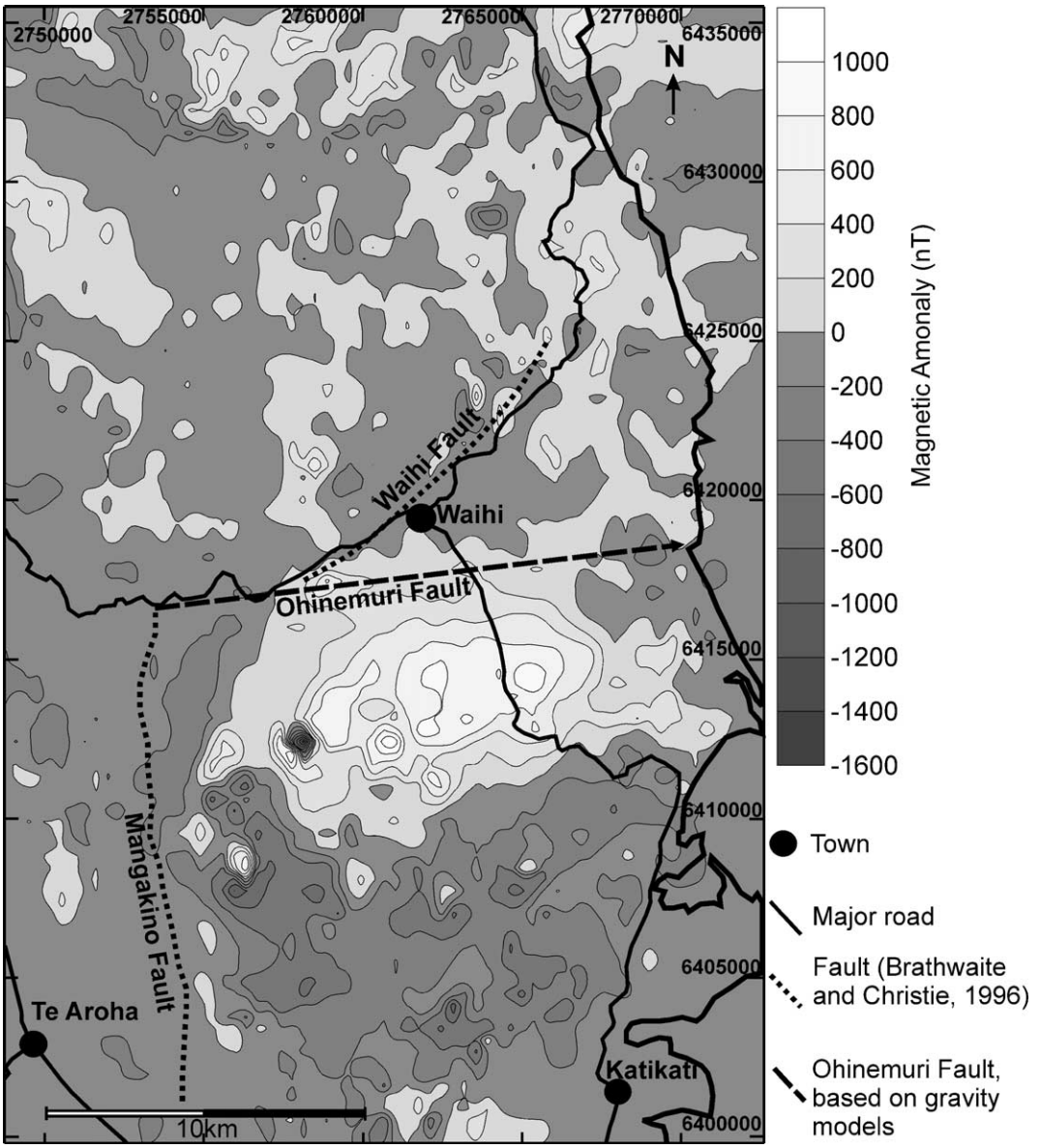

Fig. 9. Total magnetic intensity (TMI) map of the study area. The map shows gridded data from the AMOCO aeromagnetic survey of the southern Coromandel Peninsula (Couper and Lawton, 1978; Couper and O'Leary, 1980). The locations of the Ohinemuri, Waihi and Mangakino faults (Brathwaite and Christie, 1996) are shown.

Lawton (1978) proposed that this magnetic anomaly may result from a buried plutonic body estimated to be at approximately 3–4 km depth; however, any such body, surprisingly, does not appear to have an observable gravity anomaly. This contrasts with Long Valley Caldera in California (Carle, 1988) where a misfit of approximately 8 mGal between the observed gravity anomaly and the expected anomaly based on known lithology revealed the presence of a large buried plutonic body, interpreted as the crystallised root of the silicic volcanic system (Carle, 1988). Plutonic bodies are common below calderas worldwide (Lipman, 1984), and the occurrence of plutonic bodies beneath the TVZ has been suggested from aeromagnetic data (Soengkono, 1995) and deep drilling at the Ngatamariki geothermal field that intercepted a diorite pluton at 2460 m depth (Arehart et al., 1997). If the Waihi magnetic anomaly results from a pluton, it may be the magma source for the caldera-forming eruption and the large volume of volcanic rocks filling the Waihi Basin, though the pluton must be at least 7 km southeast of the proposed caldera. Alternatively, this magnetic anomaly may be related to the Ananui andesites since large domes and flows of highly magnetic 3 Ma Ananui Andesite are located directly over it, in which case the deeper body must post-date the formation of the Uretara Formation and Waihi Basin.

5.4. The relationship of epithermal deposits to the regional faults and caldera

Many of the epithermal mineral deposits in the southern Coromandel are located close to the Ohinemuri and Mangakino fault systems, which form the boundaries of the Waihi Basin, and may be the surface expression of pre-existing regional faults. Most epithermal Au–Ag deposits in the southern Hauraki Goldfield have been dated between 7.0 and 6.0 Ma (Mauk and Hall, 2004), i.e., shortly after deposition of the Waipupu Formation. Because there is no alteration in the Uretara Formation, which formed at 5.6–4.3 Ma (Brathwaite and Christie, 1996), it indicates that hydrothermal systems were active prior to its deposition. The proximity of epithermal deposits to the Ohinemuri and Mangakino faults suggests that these faults pre-date or formed at the same time as the major phase of hydrothermal activity and, thus, before caldera formation. Epithermal deposits and their associated alteration halos, although located close to these faults, are not located directly along them, and the relationships among first-order regional faults, subsidiary second-order faults and mineral deposits are complex and beyond the scope of this study.

6. Conclusions

This study shows that the Waihi Basin in the Coromandel Volcanic Zone of the North Island, New Zealand, is most probably a Miocene to Pliocene caldera whose location and collapse were controlled by pre-existing regional-scale faults. Gravity modelling has delineated the subsurface geometry of this caldera and shows it to have the form of an asymmetric trapdoor caldera with polygonal northern and western faulted margins. It contains a high proportion of very low-density rocks, possibly rhyolites or ignimbrites, the presence of which is masked by a thick overlying sequence of andesitic volcanic rocks. Although the gravity data provide no evidence for a pluton below the floor of the caldera, such a body could explain the occurrence of the large magnetic anomaly to the south, although the relationship between the source of the magnetic anomaly and the caldera remains unknown. Available data suggest that the bounding faults predated caldera formation and may have helped localize hydrothermal fluid flow that led to epithermal Au–Ag deposits.

Acknowledgements

We thank the University of Auckland and the Foundation for Research Science and Technology for financial support and Newmont Waihi Gold for access to drill core, mine and exploration data. We also thank R. Brathwaite, B. Hegan, A. Morrell, J. Rowland, M. Simpson, V. Smith, L. Torckler and C. Yong for technical assistance and valuable discussion and two anonymous reviewers for valuable comments that helped improve the manuscript.

References

Adams, C.J., Graham, I.J., Seward, D., Skinner, D.N.B., 1994. Geochronological and geochemical evolution of late Cenozoic volcanism in the Coromandel Peninsula, New Zealand. New Zealand Journal of Geology and Geophysics 37, 359–379.

Arehart, G.B., Wood, C.P., Christenson, B.W., Browne, P.R.L., Foland, K.A., 1997. Timing of volcanism and geothermal activity at Ngatamariki and Rotokawa, New Zealand. Proceedings of the 19th New Zealand Geothermal, 117–122.

Ballance, P.F., et al., 1999. Morphology and history of the Kermadec trench–arc–backarc basin–remnant arc system at 30–32′S: geophysical profile, microfossil and K–Ar data. Marine Geology 159, 35–62.

Beresford, S.W., Cole, J.W., 2000. Kaingaroa Ignimbrite, Taupo volcanic zone, New Zealand; evidence for asymmetric caldera subsidence of the Reporoa Caldera. New Zealand Journal of Geology and Geophysics 43 (3), 471–481.

Bibby, H.M., Caldwell, T.G., Davey, F.J., Webb, T.H., 1995. Geophysical evidence on the structure of the Taupo Volcanic Zone and its hydrothermal circulation. Journal of Volcanology and Geothermal Research 68, 29–58.

Brathwaite, R.L., Christie, A.B., 1996. Geology of the Waihi area, scale 1:50,000: Institute of Geolgoical and Nuclear Sciences, Geological map 21. Institute of Geological and Nuclear Sciences, 1 sheet + 64 pp.

Brathwaite, R.L., Pirajno, F., 1993. Metallogenic map of New Zealand. Institute of Geological and Nuclear Sciences Monograph, 3: 215.

Brathwaite, R.L., Christie, A.B., Skinner, D.N.B., 1989. The Hauraki Goldfield; regional setting, mineralisation and recent exploration. In: Kear, D. (Ed.), Mineral Deposits of New Zealand: Australasian Institute of Mining and Metallurgy Monograph vol. 13, pp. 45–56.

Bromley, C.J., Brathwaite, R.L., 1991. Waihi Basin structure in light of recent geophysical surveys. Proceedings of the 25th Annual Conference 1991, New Zealand Branch of the Australasian Institute of Mining and Metallurgy, pp. 225–238.

Carle, S.F., 1988. Three-dimensional gravity modeling of the geologic structure of Long Valley Caldera. Journal of Geophysical Research, B, Solid Earth and Planets 93 (11), 13237–13250.

Carter, L., et al., 2003. Demise of one volcanic zone and birth of another—a 12 m.y. marine record of major ryolitic eruptions from New Zealand. Geology 31 (6), 493–496.

Cole, J.W., Milner, D.M., Spinks, K.D., 2005. Calderas and caldera structures: a review. Earth-Science Reviews 69, 1–26.

Cordell, L., 1973. Gravity analysis using an exponential density–depth function—San Jacinto Graben, California. Geophysics 38 (4), 684–690.

Cordell, L., Long, C.L., Jones, D.W., 1985. Geophysical expression of the batholith beneath Questa Caldera, New Mexico. Journal of Geophysical Research, B, Solid Earth and Planets 90 (13), 11263–11269.

Couper, P.G., Lawton, D.C., 1978. Final report on exploration licence 33-051, Unpublished open-file company report. Ministry of Economic Development report MR350.

Couper, P.G., O'Leary, G.P., 1980. Final report on exploration licence 33-067, Unpublished open-file company report. Ministry of Economic Development report MR379.

Davey, F.J., Henrys, S.A., Lodolo, E., 1995. Asymmetric rifting in a continental back-arc environment, North Island, New Zealand. Journal of Volcanology and Geothermal Research 68, 209–238.

Ferguson, J.F., Cogbill, A.H., Warren, R.G., 1994. A geophysical–geological transect of the Silent Canyon caldera complex, Pahute Mesa, Nevada. Journal of Geophysical Research, B, Solid Earth and Planets 99 (3), 4323–4339.

Gadsby, M.R., Sporli, K.B., 1989. Structural background to Hauraki Goldfield mineralisation: a review. 11th New Zealand Geothermal Workshop, pp. 149–154.

Guillou, F.L., Burov, E.B., Milesi, J.P., 2000. Genetic links between ash-flow calderas and associated ore deposits as revealed by large-scale thermo-mechanical modeling. Journal of Volcanology and Geothermal Research 102 (3–4), 339–361.

Hallinan, S., 1993. Nonchaotic collapse at funnel calderas; gravity study of the ring fractures at Guayabo Caldera, Costa Rica. Geology (Boulder) 21 (4), 367–370.

Hatherton, T., Leopard, A.E., 1964. The densities of New Zealand rocks. New Zealand Journal of Geology and Geophysics 7, 605–625.

Hedenquist, J.W., Gakkai, S.C., 1996. Epithermal Gold Deposits: Styles, Characteristics, and Exploration. Resource Geology Special Publication, vol. 1. The Society of Resource Geology, Tokyo. 16 pp.

Hedenquist, J.W., Lowenstern, J.B., 1994. The role of magmas in the formation of hydrothermal ore deposits. Nature 370 (6490), 519–570.

Hegan, B.D., 2003. Kaimai tunnel: a geological section through an ancient volcano. In: Crawford, S., Hergraves, S. (Eds.), Geotechnics on the Edge. Institution of Professional Engineers New Zealand, Tauranga, New Zealand, pp. 65–70.

Henley, R.W., Ellis, A.J., 1983. Geothermal systems ancient and modern: a geochemical review. Earth-Science Reviews 19 (1), 1–50.

Hochstein, M.P., Ballance, P.F., 1993. Hauraki Rift; a young, active, intra-continental rift in a back-arc setting. Sedimentary Basins of the World 2, 295–305.

Hochstein, M.P., Nixon, I.M., 1979. Geophysical study of the Hauraki Depression, North Island, New Zealand. New Zealand Journal of Geology and Geophysics 22 (1), 1–19.

Hoover, D.B., Heran, W.D., Hill, P.L., 1992. The Geophysical Expression of Selected Mineral Deposit Models, United States Geological Survey Report, pp. 92–557.

Lipman, P.W., 1984. The roots of ash flow calderas in western North America; windows into the tops of granitic batholiths. Journal of Geophysical Research, B, Solid Earth and Planets 89 (10), 8801–8841.

Lipman, P.W., 1997. Subsidence of ash-flow calderas; relation to caldera size and magma-chamber geometry. Bulletin of Volcanology 59 (3), 198–218.

Malengreau, B., Skinner, D., Bromley, C., Black, P., 2000. Geophysical characterisation of large silicic volcanic structures in the Coromandel Peninsula, New Zealand. New Zealand Journal of Geology and Geophysics 43, 171–186.

Mauk, J.L., Hall, C.M., 2004. $^{40}Ar/^{39}Ar$ ages of adularia from the Golden Cross, Neavesville and Komata epithermal deposits, Hauraki Goldfield, New Zealand. New Zealand Journal of Geology and Geophysics 47, 227–231.

McKee, E.H., Hildenbrand, T.G., Anderson, M.L., Rowley, P.D., Sawyer, D.A., 1999. The silent canyon caldera complex; a three-dimensional model based on drill-hole stratigraphy and gravity inversion. U. S. Geological Survey Report, vol. 38, 6 sheets pp.

Milner, D.M., Cole, J.W., Wood, C.P., 2002. Asymmetric, multiple-block collapse at Rotorua Caldera, Taupo volcanic zone, New Zealand. Bulletin of Volcanology 64 (2), 134–149.

Rabone, S.D.C., 1987. PL 31757 Taieri 1: Progress Report for Period 8/8/84 to 8/8/87, Coromandel Peninsula. MR 538. Ministry of Economic Development, Wellington.

Reilly, W.I., 1972. New Zealand Gravity Map Series. New Zealand Journal of Geology and Geophysics, 15(1): 3–15.

Robertson, E.I., Reilly, W.I., 1960. The New Zealand primary gravity network. New Zealand Journal of Geology and Geophysics 3, 41–68.

Rytuba, J.J., McKee, E.H., 1984. Peralkaline ash flow tuffs and calderas of the McDermitt volcanic field, Southeast Oregon and north central Nevada. Journal of Geophysical Research, B, Solid Earth and Planets 89 (10), 8616–8628.

Seager, W.R., McCurry, M., 1988. The cogenetic Organ Cauldron and Batholith, south central New Mexico; evolution of a large-volume ash flow cauldron and its source magma chamber. Journal of Geophysical Research, B, Solid Earth and Planets 93 (5), 4421–4433.

Sibson, R.H., 1987. Earthquake rupturing as a mineralizing agent in hydrothermal systems. Geology 15 (8), 701–704.

Sillitoe, R.H., 1993. Epithermal models: genetic types, geometrical controls, and shallow features. Geological Association of Canada Special Paper 40, 403–417.

Sillitoe, R.H., 2000. Gold-rich porphyry deposits: descriptive and genetic models and their role in exploration and discovery. Reviews in Economic Geology 13, 315–345.

Simpson, M.P., Mauk, J.L., Hollinger, E., 2002. The Favona low-sulfidation epithermal Au–Ag deposit, Waihi, New Zealand. AusIMM Bulletin, 46–52.

Skinner, D.N.B., 1972. Subdivision and petrology of the Mesozoic rocks of Coromandel (Manaia Hill Group). New Zealand Journal of Geology and Geophysics 15, 203–227.

Skinner, D.N.B., 1986. Neogene volcanism of the Hauraki Volcanic Region. In: Smith, I.E.M. (Ed.), Late Cenozoic Volcanism in New Zealand, Bulletin. Royal Society of New Zealand, pp. 21–47.

Smith, S., 2003. Structural controls on epithermal mineralisation at the Karangahake Au–Ag deposit, Coromandel Peninsula, New Zealand. MSc Thesis, University of Auckland, Auckland, 105 pp.

Soengkono, S., 1985. Geophysical studies of the Mokai Geothermal Field. MSc Thesis, University of Auckland, Auckland, 150 pp.

Soengkono, S., 1995. A magnetic model for deep plutonic bodies beneath the central Taupo volcanic Zone, North Island, New Zealand. Journal of Volcanology and Geothermal Research 68, 193–207.

Sporli, K.B., 1987. Development of the New Zealand Microcontinent. In: Monger, J.W.H., Francheteau, J. (Eds.), Circum-Pacific Orogenic Belts and Evolution of the Pacific Ocean Basin. American Geophysical Union, Washington, DC, p. 165.

Stagpoole, V.M., Christie, A.B., Henrys, S.A., Woodward, D.J., 2001. Aeromagnetic map of the Coromandel region: total force anomalies. Institute of Geological and Nuclear Sciences geophysical map 14., Lower Hutt, New Zealand.

Stern, T.A., 1982. Seismic and gravity investigations of the Central Volcanic Region, North Island, New Zealand. PhD Thesis, Victoria University of Wellington, Wellington, 318 pp.

Stern, T.A., 1985. A back-arc basin formed within continental lithosphere: the Central Volcanic Region of New Zealand. Tectonophysics 112, 385–409.

Stern, T.A., Davey, F.J., 1987. A seismic investigation of the crust and upper mantle structure within the Central Volcanic Region of New Zealand. New Zealand Journal of Geology and Geophysics 30, 217–231.

White, D.E., 1955. Thermal springs and epithermal ore deposits. In: Bateman, A.M. (Ed.), Economic Geology, pp. 99–154.

Whitford, C.M., Lumb, J.T., 1975. A Catalogue of Physical Properties of Rocks. Volume 2: Listing by Geographic Location. Department of Scientific and Industrial Research Geophysics Division Report 106, Wellington, New Zealand.

Wilson, C.J.N., et al., 1984. Caldera volcanoes of the Taupo Volcanic Zone, New Zealand. Journal of Geophysical Research, B, Solid Earth and Planets 89 (10), 8463–8484.

Wilson, C.J.N., et al., 1995. Volcanic and structural evolution of Taupo Volcanic Zone, New Zealand: a review. Journal of Volcanology and Geothermal Research 68, 1–28.

Woodward, D.J., 1971. Sheet 3 Auckland, gravity map of New Zealand, Bouguer Anomalies. Department of Scientific and Industrial Research., Wellington N.Z.

Wright, I.C., 1993. Pre-spread rifting and heterogeneous volcanism in the southern Havre Trough backarc basin. Marine Geology 113, 179–200.